THE ASTROPHYSICAL JOURNAL, 215:541–551, 1977 July 15

SOFT X-RAY SOURCES AND SUPERNOVA REMNANTS IN CYGNUS: ROCKET AND *APOLLO-SOYUZ* RESULTS

A. F. DAVIDSEN,* R. C. HENRY, AND W. A. SNYDER
Department of Physics, The Johns Hopkins University
AND
H. FRIEDMAN, G. FRITZ, S. NARANAN,† S. SHULMAN, AND D. YENTIS
E. O. Hulburt Center for Space Research, Naval Research Laboratory
Received 1976 October 11

ABSTRACT

Soft X-ray (0.18–8 keV) observations of the Cygnus region obtained from proportional counters aboard a rocket and also on the *Apollo-Soyuz* mission are reported. We find that Cyg X-6, a source whose flux is confined to the 0.5–2.0 keV band, is a long, narrow filament oriented nearly perpendicular to the galactic plane. With an apparent length $\sim 9°$ and an estimated distance $d \gtrsim 1$ kpc, this feature has a linear dimension greater than or on the order of 150 parsecs. Its spectrum is adequately described by an exponential, with temperature $T \approx 2\text{–}4 \times 10^6$ K and $N_H \approx 5\text{–}10 \times 10^{21}$ cm^{-2}.

Another intense soft source whose flux is also confined to the 0.5–2.0 keV band has been discovered near γ Cygni. This source, designated Cyg X-7, has a spectrum characterized by $T \approx 1.5\text{–}5 \times 10^6$ K and $N_H \gtrsim 10 \times 10^{21}$ cm^{-2}. We discuss the possible association of Cyg X-7 with the supernova remnant DR 4. An interpretation of this object in terms of the standard adiabatic spherical shock wave model yields plausible values for the free parameters.

HB 21, another old supernova remnant, has not been detected as a soft X-ray source. The upper limits obtained imply that this object is much cooler than the Cygnus Loop and therefore that it is in a more advanced stage of evolution than any of the other known SNRs.

Subject headings: nebulae: supernova remnants — X-rays: sources

I. INTRODUCTION

This paper presents the results of soft X-ray observations near the galactic plane in Cygnus made with large area proportional counters launched aboard a sounding rocket and also aboard the *Apollo* spacecraft during the *Apollo-Soyuz* mission. Our observations of the well-known sources Cyg X-2 and Cyg X-3 have been described elsewhere (Shulman *et al.* 1975; Snyder *et al.* 1975). Here we discuss some lesser-known sources and possible sources whose emission is concentrated at low energies. The observations presented represent a substantial increase in sensitivity over previous soft X-ray surveys of the Cygnus region. As a result we have been able to confirm the existence of Cyg X-6 (Coleman *et al.* 1971) and find that it is an extended source. We have also discovered an intense soft source, designated Cyg X-7, which may be associated with the supernova remnant DR 4. Both of these sources have spectra indicating low temperatures ($\sim 10^{6.5}$ K) and high column densities ($\sim 10^{22}$ cm^{-2}), and consequently they are observable only in the 0.5–2.0 keV band. Details of the observations are given in § II, and the analysis of the X-ray spectra obtained is described in § III. In § IV we discuss the implications of the results in terms of the standard picture for the evolution of old supernova remnants.

II. THE OBSERVATIONS

The rocket data were obtained with two proportional counters, each of 1080 cm^2 effective area, launched aboard an Aerobee 200 at 0435 UT 1974 September 7. Each counter had a 2 μm thick Kimfol window and was filled with P-10 gas at 15.5 psia (1.07 bars). The counters were sensitive in the energy ranges 0.18–0.28 and 0.5–8 keV; pulse-height spectra over this range were recorded in 512 channels. The gain was calibrated by placing a ^{55}Fe source in the field of view of each detector from 80 to 100 s after launch and again from 288 to 300 s. One counter viewed the sky through a mechanical collimator which gave a circular field of view with 5° full width at half-maximum (FWHM) transmission, while the other counter had a 3° FWHM circular field of view. The two collimators were coaligned to within 0°.5.

The payload was pointed with an inertial attitude control system updated by an optical star-tracker, and a 35 mm camera provided information on the pointing direction every 1.3 s throughout the flight. The sequence of maneuvers during the first half of the flight is shown in Figure 1. The detectors were initially

* Alfred P. Sloan Foundation Research Fellow.
† On leave from Tata Institute of Fundamental Research.

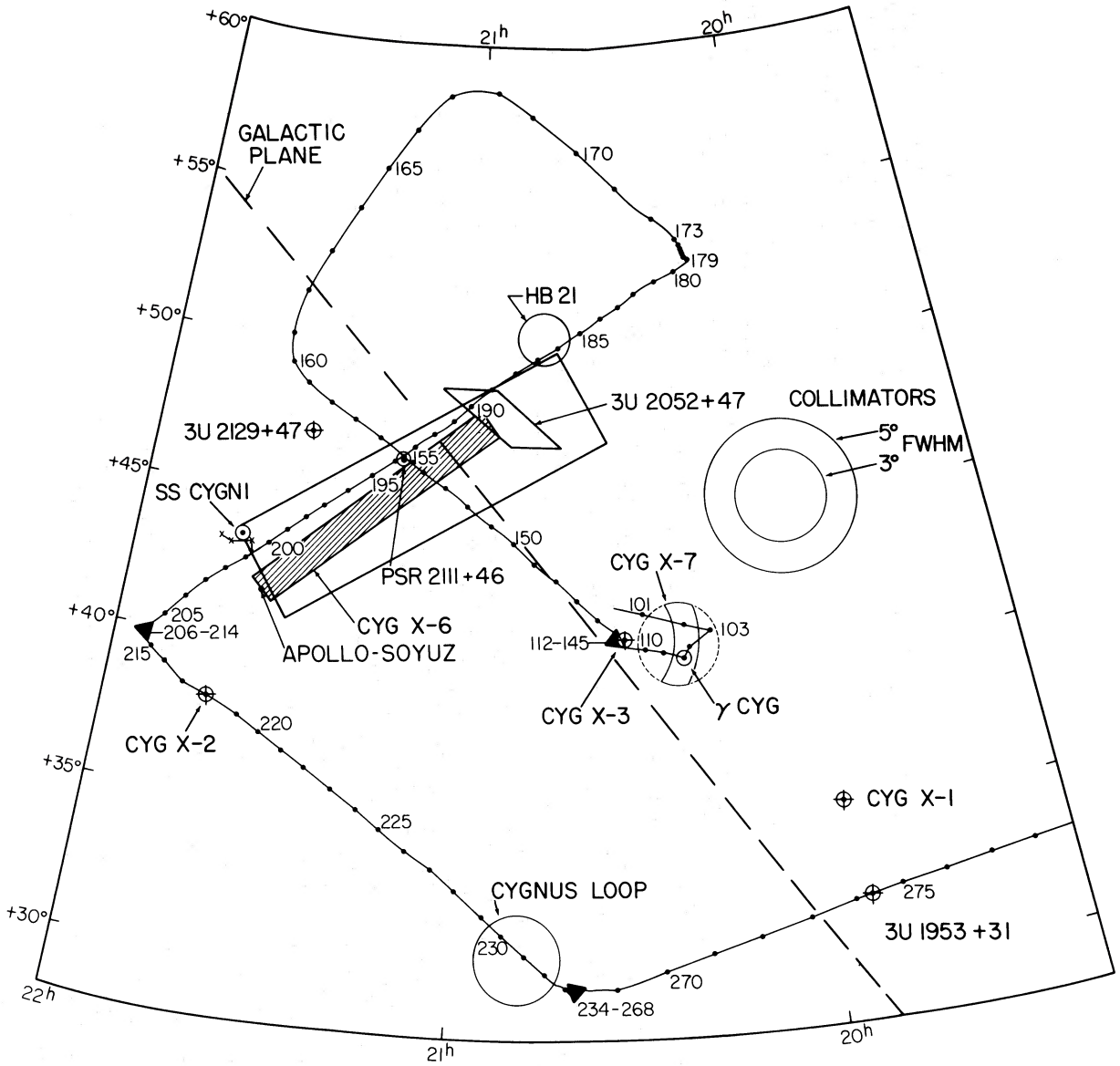

FIG. 1.—Map of the Cygnus region showing the locations of known X-ray sources and some other objects. The look direction of the rocket-borne detectors for 1 s intervals has been plotted. The look directions of the *Apollo* detector are indicated by the crosses near SS Cygni. The hatched area is an estimate of the extent of Cyg X-6 under the assumption that it is a linear feature of constant width ($\approx 1°$). The location of the new source Cyg X-7 is also indicated.

pointed perpendicular to the zenith and were then rapidly scanned to γ Cyg, which the star-tracker acquired and held from 105 to 108 s after launch. The pointing axis was then moved to Cyg X-3 and held there from 112 to 145 s. The subsequent scans through the Cygnus region are shown in Figure 1, where the pointing direction at 1 s intervals has been indicated. Additional holds occurred near Cyg X-2 and near the Cygnus Loop. Later in the flight the detectors were pointed at Her X-1, from which weak soft X-rays were detected during the nominal "off" state (Fritz *et al.* 1976). The data reported here were obtained at altitudes above 150 km, and consequently no corrections for atmospheric attenuation have been applied.

The count rates observed in each of the detectors during the maneuvers through Cygnus are displayed in Figure 2. Results for high energies ($\sim$2–8 keV), medium energies ($\sim$0.5–1.0 keV), and low energies ($\leq$0.28 keV) are shown separately for both detectors. The energy intervals have been selected to provide a clear separation of the hard and soft X-ray sources discussed below. At high energies, the initial high count rate is due to the calibration source. The count rate is then dominated by the hold on Cyg X-3 and by

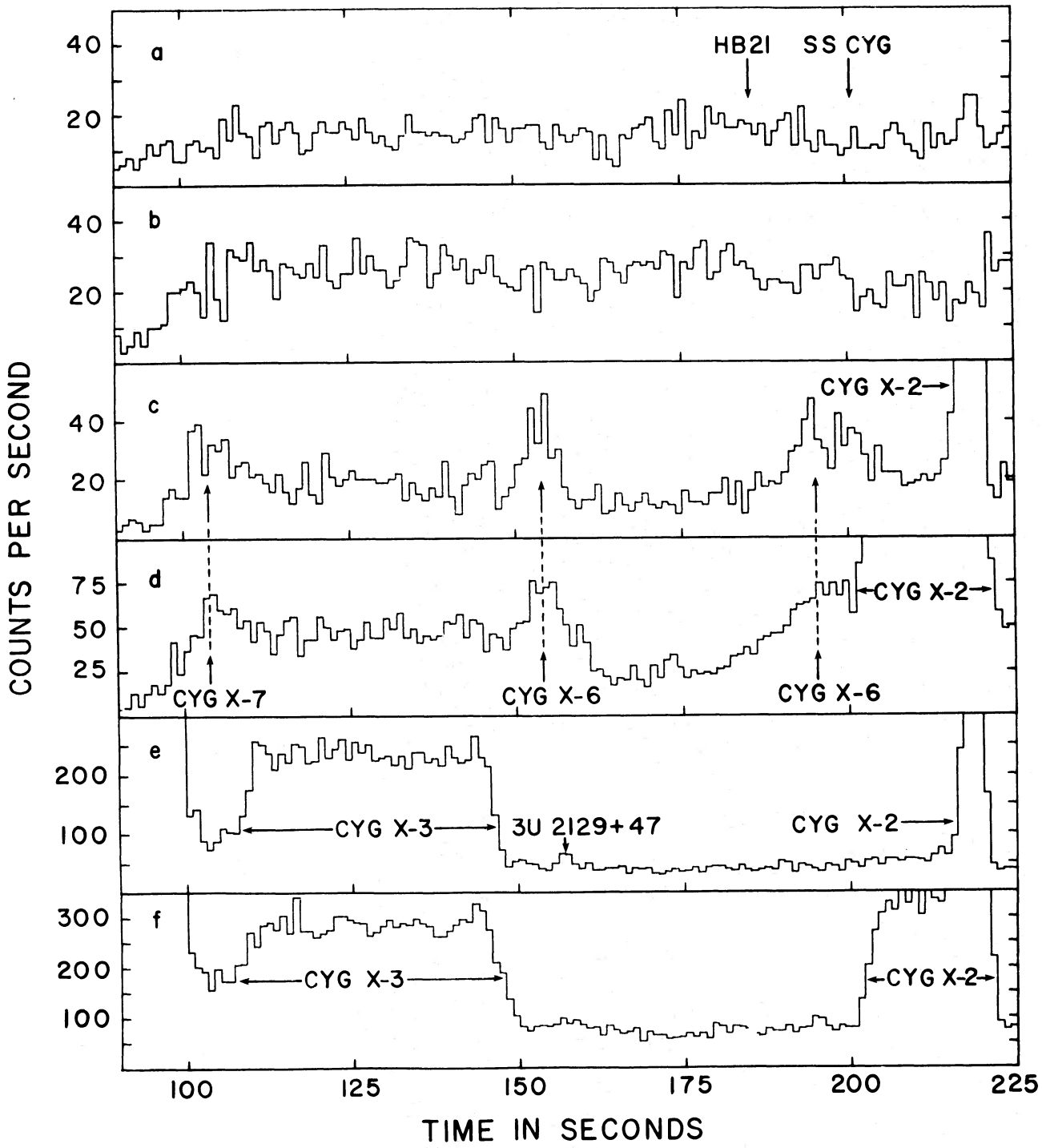

FIG. 2.—Count-rate histogram for the first half of the Aerobee rocket flight. (*a*) 0.18–0.28 keV, 3° detector; (*b*) 0.18–0.28 keV, 5° detector; (*c*) 0.5–1.0 keV, 3° detector; (*d*) 0.5–1.0 keV, 5° detector; (*e*) 2–8 keV, 3° detector; (*f*) 2–8 keV, 5° detector. The times of transit are indicated for several objects, including HB 21 and SS Cyg, which are not detected.

the hold near Cyg X-2 and subsequent transit of that source. At energies below 0.28 keV no sources at all are observed in the plotted portion of the flight, reflecting the large column densities of interstellar matter in the Cygnus direction.

The count rate in the 0.5–1.0 keV band shows an entirely different structure from either the higher or the lower energy data. In this band a source is first seen at $t = 101$ s, while the attitude control system was acquiring γ Cyg. When the detectors are pointed at Cyg X-3 (2° from γ Cyg), the count rate in the 3° FWHM detector is reduced almost to the background level observed during $t = 160$–185 s, while the count rate in the 5° FWHM detector is also reduced, but by a smaller factor. From the ratio of the count rates in the two detectors the offset of the source in the field of view can be determined. Our best estimate for the position of this new source, which we designate Cyg X-7, is shown in Figure 1. Also shown is an error circle derived from the intersection of two lines of position for a possible faint source observed in the 0.5–1.5 keV band by the Lawrence Radiation Laboratory (LRL) group (Burginyon *et al.* 1973). The radius of this circle has been taken equal to the FWHM of the LRL detector. In view of the agreement in position, spectrum, and flux (see below), we may conclude that the LRL experiment probably also detected Cyg X-7.

After the hold on Cyg X-3 (and Cyg X-7), the detectors were scanned along the galactic plane, through the center of the error box for Cyg X-6 (Coleman *et al.* 1971). In the 0.5–1.0 keV band both detectors indicate the transit of a source at $t = 154$ s, consistent with the reported Cyg X-6 position. After scanning in a loop to the north (where background data for both Cyg X-6 and Cyg X-7 were obtained from $t = 160$ to 185 s), the field of view again crossed the Cyg X-6 error box, this time perpendicular to the galactic plane. Once again a source is seen in both detectors in the 0.5–1.0 keV band, but along this direction the source is clearly extended. In the 5° detector it is first observed entering the field of view at $t \approx 184$ s, when the look direction is still well north of the galactic plane. The intensity reaches a maximum at $t = 195$ s (about 2° south of the galactic plane) in the 3° detector and then declines slowly, while the source becomes confused with Cyg X-2 in the 5° detector after $t = 201$ s. Thus the source appears to be extended from $b \approx +2°$ to $b \approx -7°$, while it is relatively narrow ($\sim 1°$) in longitude, centered at $l = 88°$. Our observations therefore suggest that Cyg X-6 is a long thin filament oriented roughly perpendicular to the galactic plane.

Cyg X-6 was also observed with the NRL X-ray experiment aboard the *Apollo-Soyuz* mission (Shulman *et al.* 1976). The detector was nearly identical to the ones employed in the rocket observation, except that the field of view was 4° FWHM. A total of 164 s of data on Cyg X-6 were obtained at 1632 UT on 1975 July 22. The detector was pointed near SS Cyg and moved through an angle of about 1° during the observation, as shown by the crosses in Figure 1. The variation of the count rate yields an estimate for the offset of the source from the center of the field of view. Assuming a line source oriented approximately perpendicular to the galactic plane and combining the *Apollo* and rocket results, we obtain the position indicated in Figure 1.

We cannot entirely exclude the possibility that Cyg X-6 actually consists of several point sources arranged along a line, but at least three sources would be required. While the northernmost one could possibly be identified with 3U 2052+47, the other two would have to be new sources, and all three would have to have the unusual soft spectrum discussed below. The alternative conclusion, which we adopt, is that Cyg X-6 is a very extended source, probably about 9° long by $\sim 1°$ wide. When combined with a minimum distance estimate based on the low-energy X-ray absorption (see below), the observations indicate Cyg X-6 is over 150 pc long.

III. X-RAY SPECTRA

a) Cygnus X-6

The pulse-height spectrum observed from Cyg X-6 in the 5° rocket detector is shown in Figure 3 (*top panel*). The flux from this source is entirely concentrated in the range 0.5–2.0 keV. The deficiency of counts near 0.25 keV is due to spatial inhomogeneity of the X-ray background at these energies, while the slight excess of counts in the 3–7 keV range is probably due to a small amount of contamination from one or more nearby hard X-ray sources, including 3U 2129+47. The histogram in Figure 3 shows the predicted response of the detector to the best-fitting exponential spectrum, $N(E) \propto E^{-1} \exp [-E/kT - \sigma(E) N_{\rm H}]$ photons cm^{-2} s^{-1} keV^{-1}, where $T = 2.5 \times 10^6$ K and $N_{\rm H} = 8.5 \times 10^{21}$ cm^{-2}, and we have employed the effective cross section $\sigma(E)$ of Brown and Gould (1970). The results obtained with the 3° detector are similar to those displayed in Figure 3.

The spectrum obtained with the *Apollo-Soyuz* instrument is also shown in Figure 3 (*bottom panel*), along with the best-fitting exponential spectrum, which has $T = 4.6 \times 10^6$ and $N_{\rm H} = 5.2 \times 10^{21}$. The *Apollo* data are contaminated by a strong line from the ^{55}Fe calibration source, but this does not interfere greatly with the observation of low-energy X-rays from Cyg X-6. These data also reveal a problem in the background subtraction at 0.25 keV which may be due to the presence of SS Cyg in the field of view. The flux observed in the *Apollo* detector is considerably lower than that observed by the rocket detectors because much of Cyg X-6 is outside the *Apollo* field of view.

The 90% confidence limits on T and $N_{\rm H}$ for all three sets of data are displayed in Figure 4. These have been calculated in accordance with the procedures described by Lampton, Margon, and Bowyer (1976). The relatively large range of acceptable values for these parameters, $T = 1.5$–7×10^6 K and $N_{\rm H} = 3$–17×10^{21} cm^{-2}, is due to the small energy range over which the flux is detectable. The temperatures obtained here are somewhat higher, while $N_{\rm H}$ is

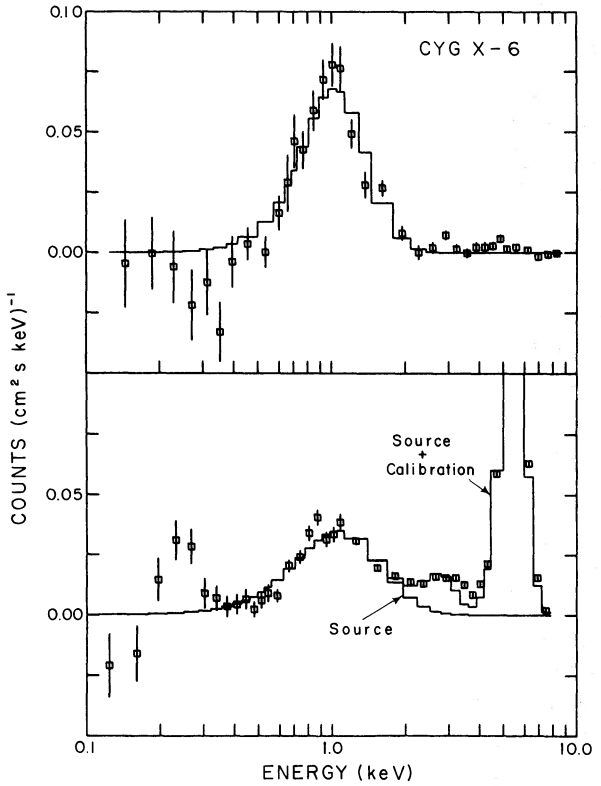

FIG. 3.—Pulse-height spectrum of Cyg X-6 observed with the 5° rocket detector (*top panel*) and with the *Apollo* detector (*bottom panel*). Plus and minus one sigma error bars are indicated. The histograms show the predicted response of the detectors to the best-fit exponential spectra. The histogram labeled "source + calibration" includes an additional line component to fit the ^{55}Fe calibration source which was jammed in place during the observation.

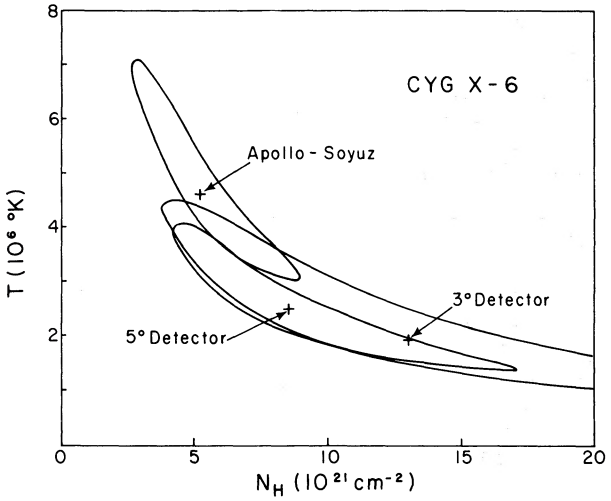

FIG. 4.—Contours indicating allowed values of T and N_H for exponential fits to the Cyg X-6 spectrum. The 90% confidence limits are drawn for the two rocket detectors and for the *Apollo-Soyuz* detector. The crosses indicate best-fit values.

somewhat lower than the corresponding values obtained by Coleman *et al.* (1971), but the similarities of the observations are more striking than these small differences. A power-law fit to the Cyg X-6 data requires a spectral index $|\alpha| \gtrsim 6$ with a best-fit spectrum $N(E) \propto E^{-9.5}$. An attempt to fit the spectrum with a single line at 1.05 keV (Coleman *et al.* 1971) yielded poor results. The most plausible conclusion is that we are dealing with a thermal source with a characteristic temperature of a few million degrees and a large interstellar column density approaching 10^{22} cm^{-2}. Incorporation of a Gaunt factor with the exponential spectrum was found to lead to values of T and N_H that did not differ significantly from those reported here. No attempt to fit the data with more complicated models for hot gas with line emission has been made.

An accurate value for the total flux from Cyg X-6 is difficult to determine from these data because the source is larger than our field of view, and yet insufficient information is available to map the surface brightness. Under the assumption that the source has the shape and position indicated in Figure 1 and uniform surface brightness, we obtain $F(0.5\text{–}2.0\ \text{keV}) \approx 4 \times 10^{-10}$ ergs cm^{-2} s^{-1}. This number should be regarded as uncertain by $\sim 50\%$. It is in good agreement with the result reported by Coleman *et al.* (1971) that $F(0.5\text{–}1.4\ \text{keV}) \approx 6 \times 10^{-10}$ ergs cm^{-2} s^{-1}.

b) Cygnus X-7

The spectrum of Cyg X-7 has been more difficult to determine because of its proximity to the strong source Cyg X-3. However, the spectra of these two sources are very different, and their relative contributions to the 3° and 5° detectors are also different. These facts allow the parameters characterizing each of the sources to be determined reasonably well, in spite of source confusion.

In Figure 5 we have displayed the pulse-height spectra obtained in both the 3° and the 5° detectors during the hold on Cyg X-3. Both sets of data show a similar peak at 4 keV, which is consistent with previous observations of Cyg X-3 (e.g., Mason, Sanford, and Ives 1975). However, the 5° detector also shows a large peak in the flux near 1 keV, while the 3° detector shows a much smaller peak at about the same energy. This low-energy peak is due to Cyg X-7, which contributes only slightly to the 3° detector data because it is near the edge of the field of view during the hold on Cyg X-3. The pulse-height spectrum obtained in the 5° detector during the star-tracker update on γ Cyg is displayed in Figure 6. At this time the relative contribution of Cyg X-7 is much larger, but the high-energy flux due to Cyg X-3 is also evident.

All of these data have been analyzed in terms of a two-component spectrum. It was found that, of the three common analytic spectral forms, only a blackbody provided an acceptable fit to the high-energy (Cyg X-3) component. The result for Cyg X-3, $T = 2.2 \times 10^7$ K and $N_H = 2.3 \times 10^{22}$ cm^{-2}, has

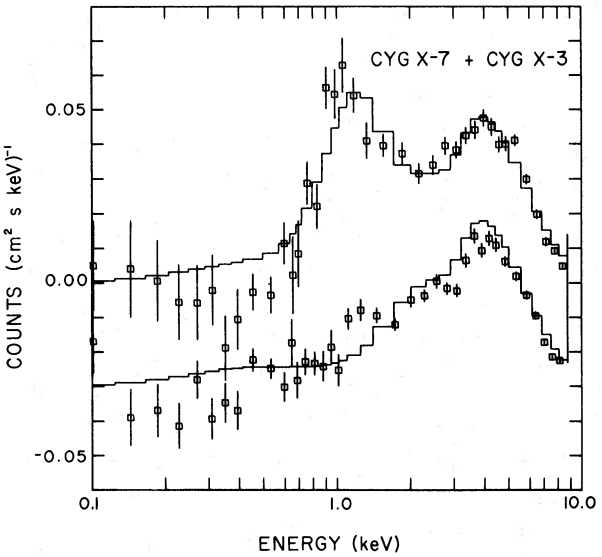

FIG. 5.—Pulse-height spectra observed while pointed at Cyg X-3 but with Cyg X-7 also in the field of view. *Upper points and curve*, 5° detector; *lower points and curve*, 3° detector, offset by −0.03. The histograms are explained in the text.

been discussed elsewhere (Shulman *et al.* 1975). We have chosen to represent the low-energy (Cyg X-7) component by an exponential spectrum (although other forms are not ruled out). The histogram in Figure 6 shows the detector response to the best-fitting two-component spectrum obtained on Cyg X-7, allowing the amplitude, temperature, and N_H to vary independently for each component. In Figure 5 the upper histogram shows the same spectrum with only the amplitudes of the two components allowed to vary. The lower histogram in Figure 5 represents the contribution of the Cyg X-3 component alone, computed for the 5° detector and compared with the 3° detector data. This curve has not been renormalized or corrected for the small gain differences between the two detectors. Thus it is not surprising that there are small systematic differences between the data and the curve. Nevertheless, this plot serves to demonstrate the consistency of the results and shows that, except for a small excess at ~1.5 keV, all of the flux in the 3° detector may be attributed to Cyg X-3.

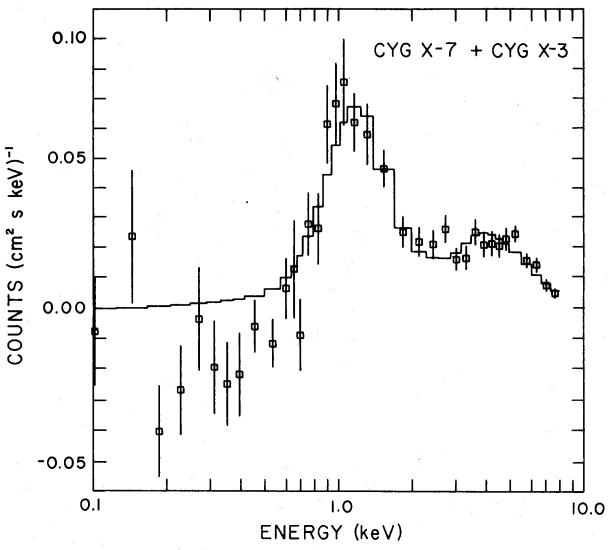

FIG. 6.—Pulse-height spectrum of Cyg X-7 in the 5° detector with a contribution at high energies due to Cyg X-3. The histogram shows the best-fit composite spectrum consisting of a blackbody for the high-energy Cyg X-3 component and an exponential spectrum for the low-energy Cyg X-7 component.

The best-fit exponential spectrum for Cyg X-7 in the 5° detector has $T = 2.1 \times 10^6$ K and $N_H = 1.7 \times 10^{22}$ cm^{-2}. The 90% confidence intervals (cf. Lampton, Margon, and Bowyer 1976) for N_H and T are given in Figure 7 for data from each of the detectors. The observed flux is $F(0.5\text{–}2.0) = 2.1 \times 10^{-10}$ ergs cm^{-2} s^{-1}, with an uncertainty of about 20%. The flux obtained by Burginyon *et al.* (1973) in the 0.5–1.5 keV band for their possible source labeled LE_1 and LE_2 is estimated as $1.2 \pm 0.8 \times 10^{-10}$ ergs cm^{-2} s^{-1}. This is in good agreement with our result and indicates that the LRL group probably also detected Cyg X-7.

IV. DISCUSSION

a) Cygnus X-7 as an Old Supernova Remnant

The location of Cyg X-7 is shown in Figure 8, superposed on a map of the 5000 MHz contours of the Cygnus X radio complex from Downes and Rinehart (1966). The dashed circle indicates the position we have deduced from the report of Burginyon *et al.* (1973), while the solid curves indicate the portion of this error circle that is consistent with our observations. The center of the new error box is at $\alpha = 20^h19^m.5$, $\delta = +40°.5$ (1950.0), and its area is about 2 square degrees. Based on their positional coincidence,

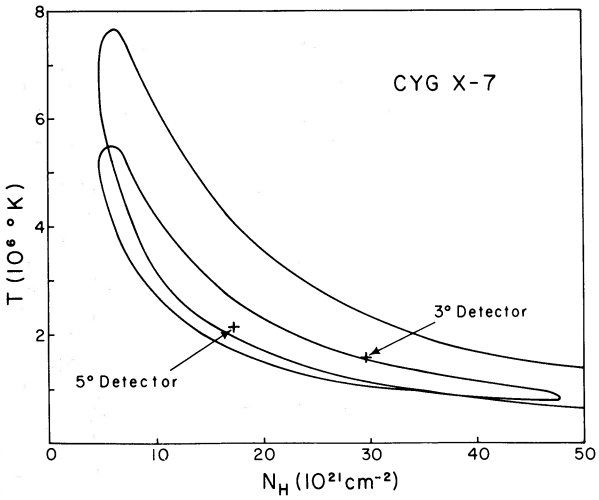

FIG. 7.—Contours indicating allowed values of T and N_H for exponential fits to the Cyg X-7 spectrum. The 90% confidence limits are drawn for the two rocket detectors. Crosses indicate best-fit values.

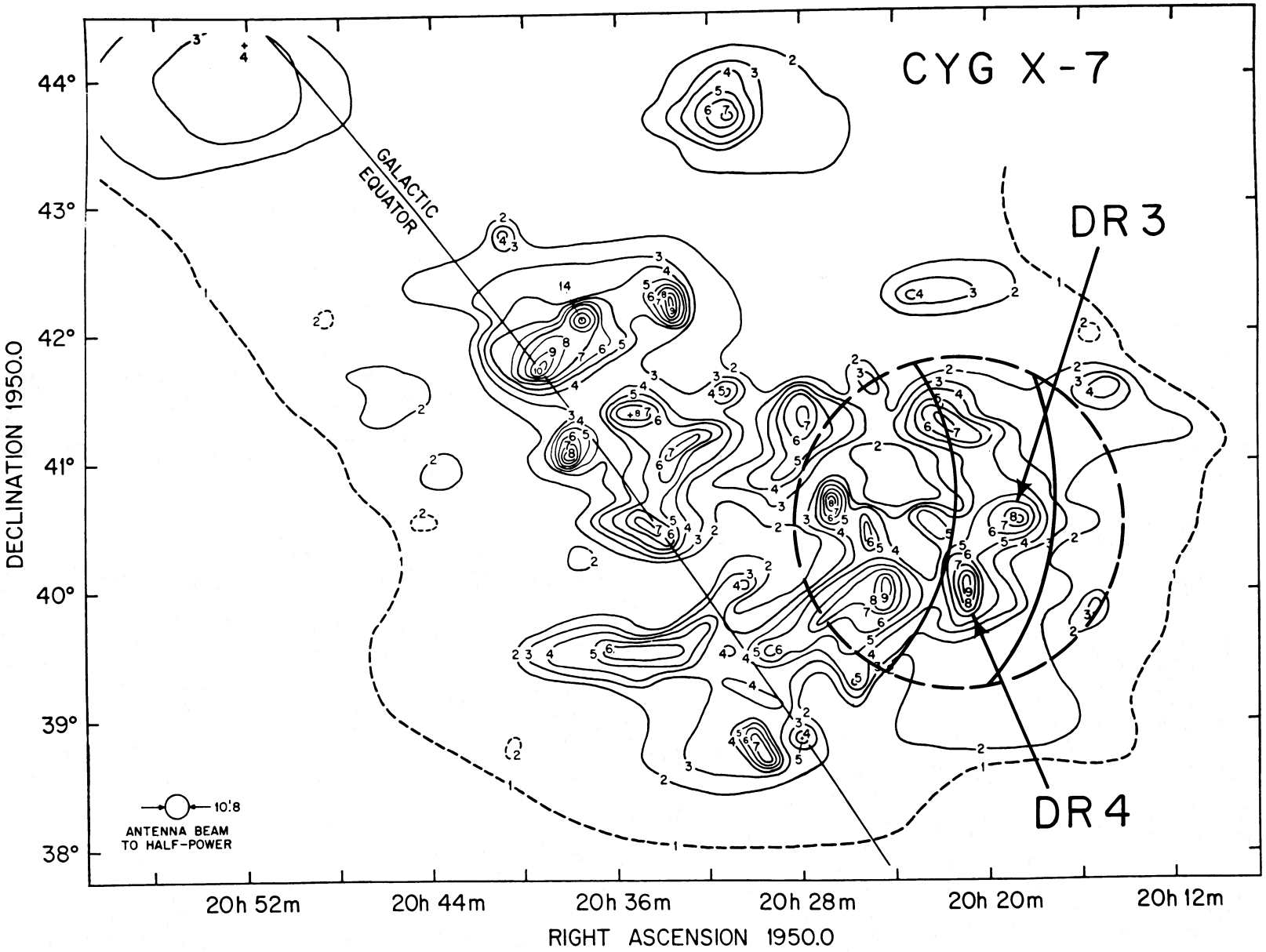

FIG. 8.—Location of Cyg X-7 superposed on the 5000 MHz contour map of the Cyg X region from Downes and Rinehart (1966). The broken circle indicates our estimate of the position based on the report of Burginyon *et al.* (1973). The solid curves indicate the region allowed by the present observation. DR 4 is a very bright supernova remnant.

the radio sources DR 3 and DR 4 are both possible counterparts of Cyg X-7.

Downes and Rinehart (1966) concluded that all of the sources which make up the Cygnus X complex are thermal with the exception of DR 4, which they observed to have a nonthermal spectrum with $\alpha = -0.7 \pm 0.3$. DR 4 is the fourth-brightest supernova remnant (SNR) at 400 MHz in the catalog of Downes (1971); its flux density of 650 Jy is exceeded only by Cas A, Vela XYZ, and the Crab. Higgs (1966) also concluded that DR 4 (=Higgs 8) is nonthermal, but found evidence that the weaker source DR 3 (=Higgs 5) is also nonthermal. Higgs suggested these two objects might actually be parts of the same SNR, which would then be at least $\sim 40'$ in extent. DR 3 is also listed as a SNR by Downes (1971) and Milne (1970) but is not included in the list of Clark and Caswell (1976) because of the detection of H 109α recombination radiation in its spectrum (Dickel and Milne 1972).

An extensive discussion of DR 4, also called the γ Cyg source because of its proximity to that star, has been given recently by Johnson (1974). He concludes that this source consists of two components. One is a SNR of $\sim 1°$ diameter, having a flux density $S(10\ \mathrm{GHz}) \approx 50$ Jy and a power-law spectral index ≈ -0.8. The other is a much smaller source (2.7 FWHM) with $S(10\ \mathrm{GHz}) \approx 10$ Jy and a harder spectrum. This small component is coincident with a small optical nebula discovered by Drake (1959). This "γ Cyg nebula," which on most photographs is buried in the halation of γ Cyg, is an H II region and not a reflection nebula (Drake 1959; Johnson 1974). It is uncertain whether the large and small sources are physically related.

Our observation that Cyg X-7 has a characteristic temperature $T \sim 3 \times 10^6$ K, similar to the Cygnus Loop and Vela SNRs, and that it lies in the direction of a radio SNR, suggests very strongly that this source is in fact a SNR. However, DR 4 was proposed as a counterpart of the possible source reported by Burginyon *et al.* (1973) and was subsequently observed with the *Copernicus* X-ray detector by Zarnecki *et al.* (1975). These authors obtained an upper limit in the 0.4–1.4 keV region a factor 10 below the inferred LRL flux of 0.06–0.09 photons $\mathrm{cm}^{-2}\ \mathrm{s}^{-1}$, but they noted the confusion which exists regarding the size of the radio source and the possibility that the SNR is considerably larger than their 13′ field of view. Although the actual pointing direction of the *Copernicus* observation was not stated, it appears that one may conclude that Cyg X-7 is not associated with the small component of DR 4 or the γ Cyg optical nebula or γ Cyg itself, but could perhaps be associated with the $\sim 1°$ diameter SNR component of DR 4 discussed by Johnson (1974). In what follows we show that this assumption leads to a consistent picture for Cyg X-7/DR 4 as an old SNR in the adiabatic expansion phase of its evolution.

The data presented here do not provide a precise determination of the temperature of the SNR, but the overlap region of acceptable parameters in Figure 7 is a long, narrow strip which can be regarded as the locus of allowed T, N_{H} pairs. For each value of T in the range ~ 1.5–5×10^6 K, there is a fairly well-defined value of N_{H} from which we may calculate the absorption-corrected flux, $F = F(\mathrm{observed}) \exp(N_{\mathrm{H}}\sigma)$, where σ is the effective cross section. If the luminosity of the source at temperature T is specified independently, e.g., from the theory of an adiabatically expanding spherical shock wave, we may calculate the distance to the source as a function of T,

$$d = [L(T)/4\pi F(T)]^{1/2}\,. \tag{1}$$

The standard model gives a luminosity in the band ΔE

$$L(\Delta E, T) \approx 5 \times 10^{56} N_1^2 R^3 P(\Delta E, T)\ \mathrm{ergs\ s^{-1}}\,, \tag{2}$$

while the temperature is given by

$$T = 8 \times 10^9 (W_{51}/N_1) R^{-3}\ \mathrm{K} \tag{3}$$

(Gorenstein, Harnden, and Tucker 1974). Here N_1 is the number density outside the expanding shock in cm^{-3}, R is the radius in parsecs, $P(\Delta E, T)$ is the cooling function, and W_{51} is the initial supernova energy release in units of 10^{51} ergs. Combining equations (2) and (3), we have

$$L(\Delta E, T) \approx 4 \times 10^{37} W_{51} N_1 T_6^{-1} P_{23}(\Delta E, T)\ \mathrm{ergs\ s^{-1}}\,, \tag{4}$$

where $T_6 = T/10^6$ K and $P_{23} = P/10^{-23}$ ergs $\mathrm{cm}^3\ \mathrm{s}^{-1}$. For the energy band ~ 0.5–1.5 keV and $2 \lesssim T_6 \lesssim 5$, we find, from Raymond, Cox, and Smith (1976), that

$$T_6^{-1} P_{23}(0.5\text{–}1.5, T) \approx \mathrm{constant} \approx 0.5\,. \tag{5}$$

Thus we have

$$L \approx 2 \times 10^{37} W_{51} N_1\ \mathrm{ergs\ s^{-1}} \tag{6}$$

over the relevant temperature range. Inserting this in equation (1), we find

$$d = 4.2 F_8^{-1/2} W_{51}^{1/2} N_1^{1/2}\ \mathrm{kpc}\,, \tag{7}$$

where $F_8 = F/10^{-8}$ ergs $\mathrm{cm}^{-2}\ \mathrm{s}^{-1}$ is the absorption-corrected flux. The diameter of the remnant obtained from equation (3) is

$$D = 40 W_{51}^{1/3} N_1^{-1/3} T_6^{-1/3}\ \mathrm{pc}\,. \tag{8}$$

When equations (7) and (8) are combined, the angular diameter is given by

$$\theta = 33 F_8^{1/2} T_6^{-1/3} W_{51}^{-1/6} N_1^{-5/6}\ \mathrm{arcmin}\,. \tag{9}$$

The dependence on W_{51} is weak, and for definiteness below we take $W_{51} = 0.4$, which is the value found for the Cygnus Loop, Vela, and Puppis SNRs (Gorenstein, Harnden, and Tucker 1974).

Results for θ as a function of T are given in Table 1 for several assumed values of N_1. The observational limits on T place limits on θ such that if $N_1 \leq 0.1$ cm^{-3}, $\theta \geq 61'$, while if $N_1 \geq 10\ \mathrm{cm}^{-3}$, $\theta \leq 23'$. The largest suggested diameter for DR 4 is $\theta \approx 60'$

TABLE 1

ANGULAR DIAMETER OF SNR MODELS FOR CYG X-7

			Θ (arcmin)				
T_6	$N_H \times 10^{-21}$	F_8	$N_1 = 0.1$	0.3	1.0	3.0	10
5.....	7.5	0.16	61	24	8.9	3.6	1.3
4.....	9	0.24	80	32	12	4.7	1.7
3.....	13	0.70	150	60	22	8.8	3.2
2.....	20	4.6	440	176	65	26	9.5
1.5....	26	23	1100	430	160	63	23

(Johnson 1974). The failure to detect X-rays with *Copernicus* (Zarnecki *et al.* 1975) suggests that $\theta \gtrsim 30'$. Thus the probable range for the true angular diameter of DR 4 is consistent with our observations of Cyg X-7 and the interpretation of DR 4/Cyg X-7 as a SNR in the adiabatic expansion phase. This statement holds for any reasonable value of W_{51} and for $0.1 \lesssim N_1 \lesssim 10\ \mathrm{cm}^{-3}$.

The constraints discussed so far involve only the X-ray data. An additional constraint on the models may be provided by assuming DR 4 is the radio counterpart of Cyg X-7. We take the flux density $S(408\ \mathrm{MHz}) = 650$ Jy (cf. Johnson 1974), and calculate the surface brightness Σ_{408} as a function of the assumed angular diameter Θ. We then use the surface brightness–diameter relation for SNRs (Clark and Caswell 1976) to obtain the diameter. Finally, the diameter and the angular diameter yield the distance. The result is

$$d = 7.47\Theta^{-1/3}, \qquad (10)$$

where d is in kpc and Θ is in arcmin. Using equations (7), (9), and (10), we calculate some specific models for Cyg X-7/DR 4. Parameters of these models are given in Table 2, where we have retained the assumption that $W_{51} = 0.4$. From Table 2 we find that the constraint that $\Theta \gtrsim 30'$ implies that the remnant is expanding into a region of ambient density $\lesssim 1\ \mathrm{cm}^{-3}$. The distance to the remnant is ~ 2 kpc and the average density along the line of sight is $\sim 2\ \mathrm{cm}^{-3}$. Both the observed column density and the derived space density are consistent with 21 cm observations in directions near DR 4 (Kaftan-Kassim 1961), which lies along the tangent to the Cygnus spiral arm. The models are also self-consistent in that the calculated diameters are smaller than the critical diameters where radiative losses become important (Cox 1972), so that the assumption that the SNR is in the adiabatic phase is justified. The derived age of the SNR is $\sim 10^4$ years.

TABLE 2

MODEL PARAMETERS FOR CYG X-7/DR 4 AS A SNR

N_1 (cm^{-3})	0.1	1.0	10
Θ (arcmin).....	84	33	13
d (kpc).....	1.7	2.4	3.2
D (pc).....	42	22	12
T (10^6 K).....	3.6	2.3	1.6
N_H (10^{21} cm^{-2}).....	10	18	25
$\langle n_H \rangle$.....	2.0	2.5	2.6

The assumption that Cyg X-7 is associated with DR 4 and that this object is a SNR in the adiabatic expansion phase leads to plausible results for all of the parameters involved in the model. In particular, the object appears to be quite similar to nearer and better observed objects such as the Cygnus Loop. A test of the model will require a better determination of the temperature as well as a measurement of the angular size of the X-ray source.

b) Cygnus X-6

After the first report of this source by Coleman *et al.* (1971), several other experimenters failed to confirm its existence (e.g., Borken, Doxsey, and Rappaport 1972; Burginyon *et al.* 1973). In the light of the present result that Cyg X-6 is very extended, however, these negative results no longer appear contradictory.

Both its morphology and its soft spectrum suggest that Cyg X-6 may be similar to the North Polar Spur (Bunner *et al.* 1972; de Korte *et al.* 1974; Cruddace *et al.* 1976). However, the location of Cyg X-6 does not correlate very well with any of the known radio loops (Haslam, Kahn, and Meaburn 1971). It lies about 10° outside the small circle continuation of Loop III and about 20° inside the small circle continuation of Loop II and is not parallel to either one of them.

The high column density required to fit the Cyg X-6 spectrum suggests that its distance is considerably greater than those usually ascribed to the radio loops. With N_H in the range $5\text{–}10 \times 10^{21}\ \mathrm{cm}^{-2}$, a mean density of $1\ \mathrm{cm}^{-3}$ would imply a distance of 1.6–3.2 kpc. The star 68 Cyg lies very close to the direction to Cyg X-6 and yields a Lα column density of 1.5×10^{21} ($+100\%$, -50%) for a distance of 720 pc (Savage and Jenkins 1972). This gives a mean density $n_H = 0.7\ \mathrm{cm}^{-3}$, with an upper limit of $1.4\ \mathrm{cm}^{-3}$. The corresponding lower limit on the distance to Cyg X-6 is 1.1 kpc. However, if a substantial fraction of the interstellar medium in this direction is in a form other than neutral hydrogen, this minimum distance could be reduced.

When corrected for absorption, the observed flux from Cyg X-6 yields a luminosity $L(0.5\text{–}2\ \mathrm{keV}) = 2 \times 10^{36} d^2$ ergs s^{-1}, where d is the distance in kpc. The length of the source corresponding to its $\sim 9°$ extent is $l \approx 157d$ pc and its width ($\sim 1°$) is $w \approx 17d$ pc. If we assume the smaller dimension is also characteristic of its depth along the line of sight (i.e., the source is a prolate ellipsoid), the volume is $V \approx 5 \times 10^{59} d^3\ \mathrm{cm}^3$. The emissivity is then $j(0.5\text{–}2\ \mathrm{keV}) \approx 0.4 \times 10^{-23} d^{-1}$ ergs $\mathrm{cm}^{-3}\ \mathrm{s}^{-1}$. Since the cooling coefficient at $\sim 3 \times 10^6$ K is $\sim 2 \times 10^{+23}$ ergs $\mathrm{cm}^3\ \mathrm{s}^{-1}$ (Raymond, Cox, and Smith 1976), the required density in the source is $\sim 0.4 d^{-1/2}\ \mathrm{cm}^{-3}$.

The true nature of Cyg X-6 is still unclear. Its temperature, luminosity, and extended size all suggest that

TABLE 3

COMPARISON OF THE CYGNUS LOOP AND HB 21

Parameters	Cygnus Loop	HB 21
S_{408} (Jy)	$+316$	$+371$
Θ (arcmin)	$+180$	$+100$
α	-0.45	-0.40
Σ_{408} (W m^{-2} Hz^{-1} sr^{-1})	$+1.46 \times 10^{-21}$	$+5.56 \times 10^{-21}$
D (pc)	$+43.6$	$+38.1$*
d (kpc)	$+0.8$	$+1.3$*
z (pc)	-120	$+107$*
N_H (cm^{-2})	$+5.2 \times 10^{20}$	$< 5 \times 10^{21}$
F_x (0.5–2 keV)(ergs cm^{-2} s^{-1})	$+9 \times 10^{-9}$	$< 4 \times 10^{-11}$
L_x (0.5–2 keV)(ergs s^{-1})	$+6 \times 10^{35}$	$< 4.8 \times 10^{34}$*
T_x (K)	$+3.1 \times 10^{6}$	$< 2 \times 10^{6}$

NOTE.—Quantities marked with an asterisk have been derived from the Σ–D relation of Clark and Caswell (1976).

it is an old supernova remnant, but its apparently very elongated form and its large linear dimension set it apart from other soft X-ray–emitting SNRs. Perhaps it is related to the hot tunnels in the interstellar medium proposed by Cox and Smith (1974). Alternatively, it may represent a rising column of hot gas escaping from the galactic disk, as in the "galactic fountain" discussed by Shapiro and Field (1976). The brightness distribution of Cyg X-6, which seems to be its most unusual feature, is not adequately determined by the present data, and a map of the 0.5–2.0 keV emission from this region is needed.

c) HB 21

The old supernova remnant HB 21 appears to be quite similar to the Cygnus Loop in a number of respects (see Table 3), and it might therefore be expected to be an intense source of soft X-rays also. In fact, Burginyon *et al.* (1973) have suggested it as a possible identification for a soft X-ray source tentatively detected on a single scan through the Cygnus region. The flux attributed to this source by Burginyon *et al.* is comparable to that which they observed from the source we have designated Cyg X-7.

Application of the standard adiabatic shock wave model also leads to the prediction that HB 21 should be a strong soft X-ray source (Clark and Culhane 1976). These authors predict a temperature $T = 4 \times 10^6$ K and a flux of 4.15×10^{-9} ergs cm^{-2} s^{-1} in the 0.5–1.5 keV band, assuming no interstellar absorption.

The rocket X-ray detectors were scanned over HB 21 (see Fig. 1) at a rate of 1 degree per second and no source was detected. Our 2 σ upper limit on the flux is $F(0.5\text{–}1.5) \leq 4.1 \times 10^{-11}$ ergs cm^{-2} s^{-1}, a factor of 100 below the predicted value (Clark and Culhane 1976). Even if we allow for the maximum interstellar absorption in this direction, $N_H \approx 5 \times 10^{21}$ cm^{-2} (Kaftan-Kassim 1961), the corrected limit is $\leq 2.4 \times 10^{-10}$ ergs cm^{-2} s^{-1}, still more than an order of magnitude below the predicted flux. In the 1.5–8.0 keV band, Clark and Culhane predict a flux of 9×10^{-11} ergs cm^{-2} s^{-1}, while our upper limit is 8×10^{-12} ergs cm^{-2} s^{-1} (1×10^{-11} corrected for absorption).

It is clear that the X-ray flux from HB 21 above 0.5 keV is much lower than that expected on the basis of the standard adiabatic shock wave model with $T \approx 4 \times 10^6$ K. However, the predicted temperature was obtained from equation (3), taking $W_{51}/N_1 = 3$ and the radius R implied by the radio Σ–D relation. If any of the parameters W_{51}, N_1, or R is adjusted to yield $T < 2 \times 10^6$ K in equation (3), then the standard model is still consistent with our data. This upper limit on the temperature of HB 21 is lower than that of any other known SNR (cf. Gorenstein and Tucker 1976). We therefore conclude that HB 21 is in a more advanced stage of evolution than any of these other SNRs and that it may even have completed the adiabatic phase and entered the radiative phase. Additional support for this conclusion is provided by the observation of an expanding shell of neutral hydrogen around HB 21 (Assousa and Erkes 1973). Such shells are expected for SNRs in the radiative phase (Chevalier 1974; Mansfield and Salpeter 1974), although the occurrence of the shell well outside the radio continuum and optical emission regions (Assousa and Erkes 1973) is not in agreement with the theoretical prediction. No H I shell has been found around the Cygnus Loop (deNoyer 1975), but the 21 cm survey by Heiles (1976) has revealed a large number of features which may be interpreted as expanding shells. The best example of such a shell (Heiles 1976) surrounds the soft X-ray hot spot in Eridanus, which we have previously interpreted as an old SNR (Naranan *et al.* 1976).

The rocket observations were supported in part by a grant from the National Aeronautics and Space Administration, and the *Apollo* observations were supported under contract T-845C with NASA/Johnson Space Center. A. F. D. is grateful for the support of the Alfred P. Sloan Foundation.

REFERENCES

Assousa, G. F., and Erkes, J. W. 1973, *A.J.*, **78**, 885.
Borken, R., Doxsey, R., and Rappaport, S. 1972, *Ap. J. (Letters)*, **178**, L115.
Brown, R. L., and Gould, R. J. 1970, *Phys. Rev. D.*, **1**, 2252.
Bunner, A. N., Coleman, P. L., Kraushaar, W. L., and McCammon, D. 1972, *Ap. J. (Letters)*, **172**, L67.
Burginyon, G., Hill, R., Palmieri, T., Scudder, J., Seward, F., Stoering, J., and Toor, A. 1973, *Ap. J.*, **179**, 615.
Chevalier, R. 1974, *Ap. J.*, **188**, 501.
Clark, D. H., and Caswell, J. L. 1976, *M.N.R.A.S.*, **174**, 267.
Clark, D. H., and Culhane, J. L. 1976, *M.N.R.A.S.*, **175**, 573.
Coleman, P. L., Bunner, A. N., Kraushaar, W. L., and McCammon, D. 1971, *Ap. J. (Letters)*, **170**, L47.
Cox, D. P. 1972, *Ap. J.*, **178**, 159.
Cox, D. P., and Smith, B. W. 1974, *Ap. J. (Letters)*, **189**, L105.
Cruddace, R. G., Friedman, H., Fritz, G., and Shulman, S. 1976, *Ap. J.*, **207**, 888.
de Korte, P. A. J., Bleeker, J. A. M., Deerenberg, A. J. M., Tanaka, Y., and Yamashita, K. 1974, *Ap. J. (Letters)*, **190**, L5.
deNoyer, L. K. 1975, *Ap. J.*, **196**, 479.
Dickel, J. R., and Milne, D. K. 1972, *Australian J. Phys.*, **25**, 539.
Downes, D. 1971, *A.J.*, **76**, 305.
Downes, D., and Rinehart, R. 1966, *Ap. J.*, **144**, 937.
Drake, F. 1959, in *Paris Symposium on Radio Astronomy*, ed. R. N. Bracewell (Stanford: Stanford University Press), p. 339.
Fritz, G., Naranan, S., Shulman, S., Yentis, D., Friedman, H., Davidsen, A., Henry, R., and Snyder, W. 1976, *Ap. J. (Letters)*, **207**, L29.
Gorenstein, P., Harnden, F. R., and Tucker, W. H. 1974, *Ap. J.*, **192**, 661.
Gorenstein, P., and Tucker, W. H. 1976, *Ann. Rev. Astr. Ap.*, **14**, 373.
Graham, D. A., Mehold, U., Hesse, K. H., Hills, D. L., and Wielebinski, R. 1975, *Astr. Ap.*, **37**, 405.
Haslam, C. G. T., Kahn, F. D., and Meaburn, J. 1971, *Astr. Ap.*, **12**, 388.
Heiles, C. 1976, *Ap. J. (Letters)*, **208**, L137.
Higgs, L. A. 1966, *M.N.R.A.S.*, **132**, 67.
Johnson, H. M. 1974, *Ap. J.*, **194**, 337.
Kaftan-Kassim, M. A. 1961, *Ap. J.*, **133**, 821.
Lampton, M., Margon, B., and Bowyer, S. 1976, *Ap. J.*, **208**, 177.
Mansfield, V. N., and Salpeter, F. E. 1974, *Ap. J.*, **190**, 305.
Mason, K. O., Sanford, P., and Ives, J. 1975, *Goddard Symposium on X-Ray Binaries* (NASA SP-389), p. 255.
Milne, D. K. 1970, *Australian J. Phys.*, **23**, 425.
Naranan, S., Shulman, S., Friedman, H., and Fritz, G. 1976, *Ap. J.*, **208**, 718.
Raymond, J. C., Cox, D. P., and Smith, B. W. 1976, *Ap. J.*, **204**, 290.
Savage, B. D., and Jenkins, E. B. 1972, *Ap. J.*, **172**, 491.
Shapiro, P. R., and Field, G. B. 1976, *Ap. J.*, **205**, 762.
Shulman, S., Friedman, H., Fritz, G., Yentis, D., Snyder, W., Davidsen, A., and Henry, R. 1975, *Goddard Symposium on X-Ray Binaries* (NASA SP-389), p. 285.
Shulman, S., Fritz, G., Yentis, D., Cruddace, R. G., Friedman, H., Snyder, W., and Henry, R. C. 1976, *Apollo-Soyuz Preliminary Science Report* (NASA TM X-58173), p. 3–1.
Snyder, W. A., Henry, R. C., Davidsen, A. R., Shulman, S., Fritz, G., and Friedman, H. 1975, *Bull. AAS*, **7**, 505.
Taylor, J. H., and Manchester, R. N. 1975, *A.J.*, **80**, 794.
Zarnecki, J. C., Stark, J. P., Charles, P. A., and Culhane, J. L. 1975, *M.N.R.A.S.*, **173**, 103.

A. F. DAVIDSEN, R. C. HENRY, and W. A. SNYDER: Department of Physics, The Johns Hopkins University, Baltimore, MD 21218

H. FRIEDMAN, G. FRITZ, S. SHULMAN, and D. YENTIS: Code 7129, Naval Research Laboratory, Washington, DC 20375

S. NARANAN: Tata Institute of Fundamental Research, Bombay 400-005, India